Biosensors and Bioelectronics 75 (2016) 222–231

Contents lists available at ScienceDirect

Biosensors and Bioelectronics

journal homepage: www.elsevier.com/locate/bios

Highly sensitive optical fibre long period grating biosensor anchored with silica core gold shell nanoparticles

L. Marques [a], F.U. Hernandez [a], S.W. James [b], S.P. Morgan [a], M. Clark [a], R.P. Tatam [b], S. Korposh [a,b,*]

[a] Applied Optics Group, Faculty of Engineering, University of Nottingham, Nottingham NG7 2RD, UK
[b] Engineering Photonics, Cranfield University, Cranfield, Bedfordshire MK43 0AL, UK

ARTICLE INFO

Article history:
Received 21 June 2015
Received in revised form
19 August 2015
Accepted 20 August 2015
Available online 22 August 2015

Keywords:
Long period grating
Biosensor
Antigen–antibody
Silica-gold core/shell nanoparticles
Layer-by-layer

ABSTRACT

An optical fibre long period grating (LPG), modified with a coating of silica core gold shell (SiO_2:Au) nanoparticles (NPs) deposited using the layer-by-layer method, was employed for the development of a biosensor. The SiO_2:Au NPs were electrostatically assembled onto the LPG with the aid of a poly(allylamine hydrochloride) (PAH) polycation layer. The LPG sensor operates at the phase matching turning point to provide the highest sensitivity. The SiO_2:Au NPs were modified with biotin, which was used as a ligand for streptavidin (SV) detection. The sensing mechanism is based on the measurement of the refractive index change induced by the binding of the SV to the biotin. The effect on sensitivity of increasing the surface area by virtue of the SiO_2:Au nanoparticles' diameter and film thickness was studied. The lowest measured concentration of SV was 2.5 nM, achieved using an LPG modified with a 3 layer (PAH/SiO_2:Au) thin film composed of SiO_2 NPs of 300 nm diameter with a binding constant of $k = 1.7$ $(pM)^{-1}$, sensitivity of 6. 9 nm/$\left(ng/mm^2\right)$ and limit of detection of 19 pg/mm^2.

1. Introduction

Fast, reliable and highly sensitive detection of proteins and antigen–antibody reaction kinetics are desired in biology and medicine because it can facilitate prompt disease diagnosis. The presence of various proteins, or changes in their concentration, can be linked with alterations in physiology and act as an indicator of problems in the organism (Wulfkuhle et al., 2003). The quantitative detection of such proteins is conducted mainly using surface plasmon resonance (SPR), planar waveguides (Orgovan et al., 2014) and various immunoassays, providing sensitivity typically down to pg/mL (Homola, 2008). In spite of its high sensitivity, the main disadvantage of the SPR sensor is its price and real life applicability. A recent fabrication breakthrough in planar waveguides allows the use of grating coupled interferometry to achieve extremely high sensitivities to refractive index (RI) change in the order of 10^{-7} and a protein surface coverage sensitivity of 0.1 pg/mm^2 (Patko et al., 2012). In spite of the high sensitivity, their practicability for in vivo measurements remains limited. In this regard, optical fibre sensors modified with thin functional coatings offer a promising alternative to facilitate highly sensitive, selective and fast measurement in real time with the reported resolution of RI change of 10^{-6} (Korposh et al., 2012b).

Among various optical fibre sensors designs and measurements schemes, refractometers and chemical sensors based on optical fibre gratings have been employed extensively, in part because they offer wavelength-encoded information, which overcomes the referencing issues associated with intensity based approaches. A long period grating (LPG) is a core-cladding mode coupling device, where the in-fibre grating has a period of order 100–500 μm, Fig. 1a and b. The high attenuation of the cladding modes results in the transmission spectrum of the optical fibre containing a series of resonance bands centred at discrete wavelengths, with each attenuation band corresponding to the coupling to a different cladding mode, Fig. 1c. Fibre gratings facilitate the controlled coupling of light between modes of the optical fibre structure at specific resonant wavelengths, with the resonant wavelength showing sensitivity to perturbation of the fibre. Such devices have been used extensively as sensors (Grattan and Meggitt, 1999; James and Tatam, 2003, 2006).

Similar to SPR and planar waveguide devices, LPG sensors can provide highly precise analytical information about adsorption and desorption processes associated with the RI and thickness of the sensing layer. For instance, the sensitivity of LPG sensors (ca. 1 nM for antigen–antibody reactions) has been demonstrated to be of the same order of magnitude as SPR sensors (Homola, 2008; DeLisa et al., 2000). The high sensitivity of LPG based optical fibre

* Corresponding author at: Applied Optics Group, Faculty of Engineering, University of Nottingham, Nottingham NG7 2RD, UK. Fax: +44 1159515616.
E-mail address: s.korposh@nottingham.ac.uk (S. Korposh).

http://dx.doi.org/10.1016/j.bios.2015.08.046

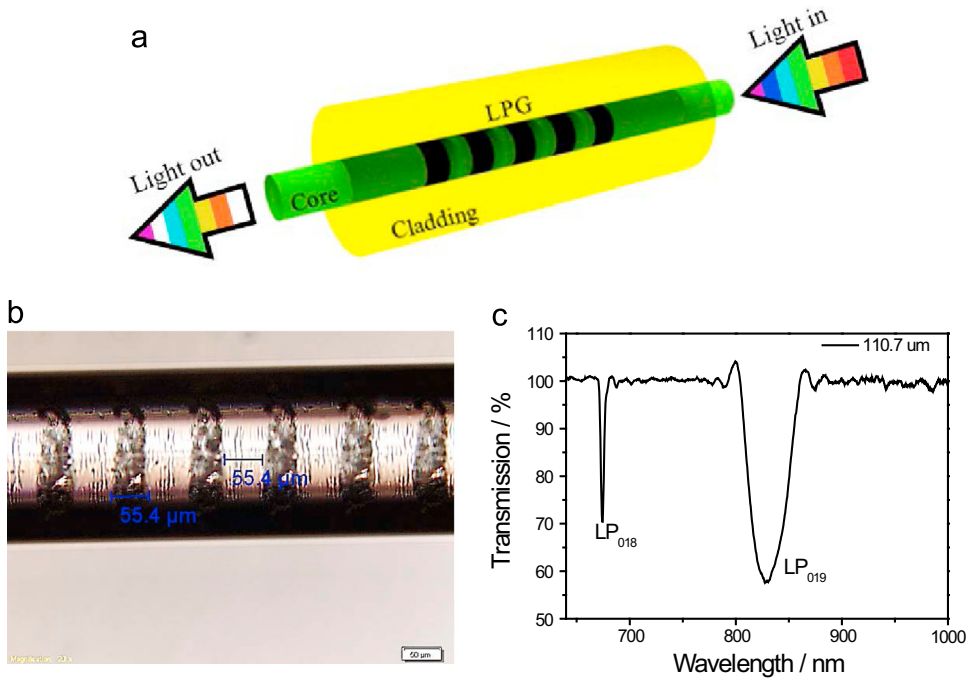

Fig. 1. (a) Schematic illustration of the LPG optical fibre; (b) optical image of the LPG written in the plastic jacket of the optical fibre; and (c) transmission spectrum (TS) of the LPG optical fibre operating at phase matching turning point (PMTP) with the grating period of 110.7 μm measured in air.

sensors operating at the phase matching turning point (PMTP) to RI change provides a high potential for detection of clinical analytes (Mishra et al., 2011). One of the earliest applications of an LPG to label free immunoglobulin (IgG) detection was demonstrated by DeLisa et al. (2000). The LPG was modified with goat anti-human IgG (antibody) and detection of specific antibody/antigen binding was investigated in the range of the concentrations of 2–100 μg/mL. Pilla et al. (2012) recently demonstrated an LPG immunosensor operating at the PMTP that provided a sensor with high sensitivity of 5 pg/mm^2 to anti-IgG analyte. Wang et al. (2009) used layer-by-layer (LbL) electrostatic self-assembly method for the deposition of polyion materials of poly(allylamine hydrochloride) and poly{1-[4-(3-carboxy-4-hydroxyphenylazo)-benzensulfonamido]-1,2-ethanediyl, sodium salt} onto the surface of the LPG with the aim of developing a biosensor using biotin–streptavidin as a demonstration bioconjugate pair. The lowest detected concentration of streptavidin was 12.5 μg/mL. Bandara et al. (2015) recently reported the detection of methicillin-resistant staphylococci using a biosensor assay consisting of nanoscale films deposited onto an LPG.

The characteristics of optical fibre sensors, such as sensitivity, response/recovery times and especially selectivity, depend strongly on the performance capabilities and the properties of the functional layer. Research in the field of optical fibre sensors (OFS) has focused on the development of new materials that can be used as sensitive elements. In this work, a novel biosensor based on an LPG coated with SiO_2:Au core/shell NPs is demonstrated with sensitivity to streptavidin of an order of magnitude greater than previously reported with LPG sensors (Wang et al., 2009). This paper expands research results presented originally as an extended abstract at OFS 23 (Marques et al., 2014) and provides a more detailed study on the effect of the SiO_2 NPs' diameter and on the presence of Au NPs. Two sets of SiO_2:Au NPs of diameters 80 and 300 nm were used to generate coatings of different layer thickness and surface areas on the LPG sensing platform. The use of a SiO_2:Au NP complex brings several advantages to biosensor development. For example, the diameter and number of Si and Au NPs can be controlled to optimise sensitivity. The Au NPs can be functionalised with different molecules, such as proteins, to provide sensor selectivity. The Au NPs' surface plasmon resonance (SPR) can then be linked to the presence or absence of target molecules. Controlling the size of the Au NPs means that the sensor can operate within a working window of 700–900 nm, which allows for optimum penetration of light across samples such as physiological fluids. A further advantage is that, since the Au NPs are covalently bonded to the Si NP surface, the system is stable and is not affected over time by washing processes.

SiO_2 NPs on the other hand have two important functions: (i) they endow the sensitive layer of the sensor with higher porosity and thus larger surface area and (ii) they optimise the efficiency of the interaction between evanescent wave and sensitive layer via optimisation of the sensitive layer thickness. Both factors are contributing to the increase of the sensitivity of the sensor. For example, it was observed that coating the optical fibre without SiO_2 nanoparticles resulted in a reduction in sensitivity by a factor of 2 (Kodaira et al., 2008).

The biotin–streptavidin interaction was used as a model system to characterise performance. The biotin is attached directly to the Au shell of the SiO_2 NPs, providing a sensor with high selectivity for protein detection. The selectivity of the sensor towards particular protein of interest can be tailored simply by changing the nature of the ligand, making LPGs modified with SiO_2:Au NPs a generic sensing platform for biosensor development.

2. Theory

2.1. LPG operation

The wavelengths at which light is coupled from the core to the cladding modes is governed by the phase matching equation

$$\lambda_i = (n_{\text{core}} - n_{\text{clad}(i)})\Lambda \quad (1)$$

where λ_i represents the wavelength at which light is coupled to the linearly polarised (LP_{0i}) cladding mode (where i =1,2,3…), n_{core} is the effective refractive index of the mode propagating in

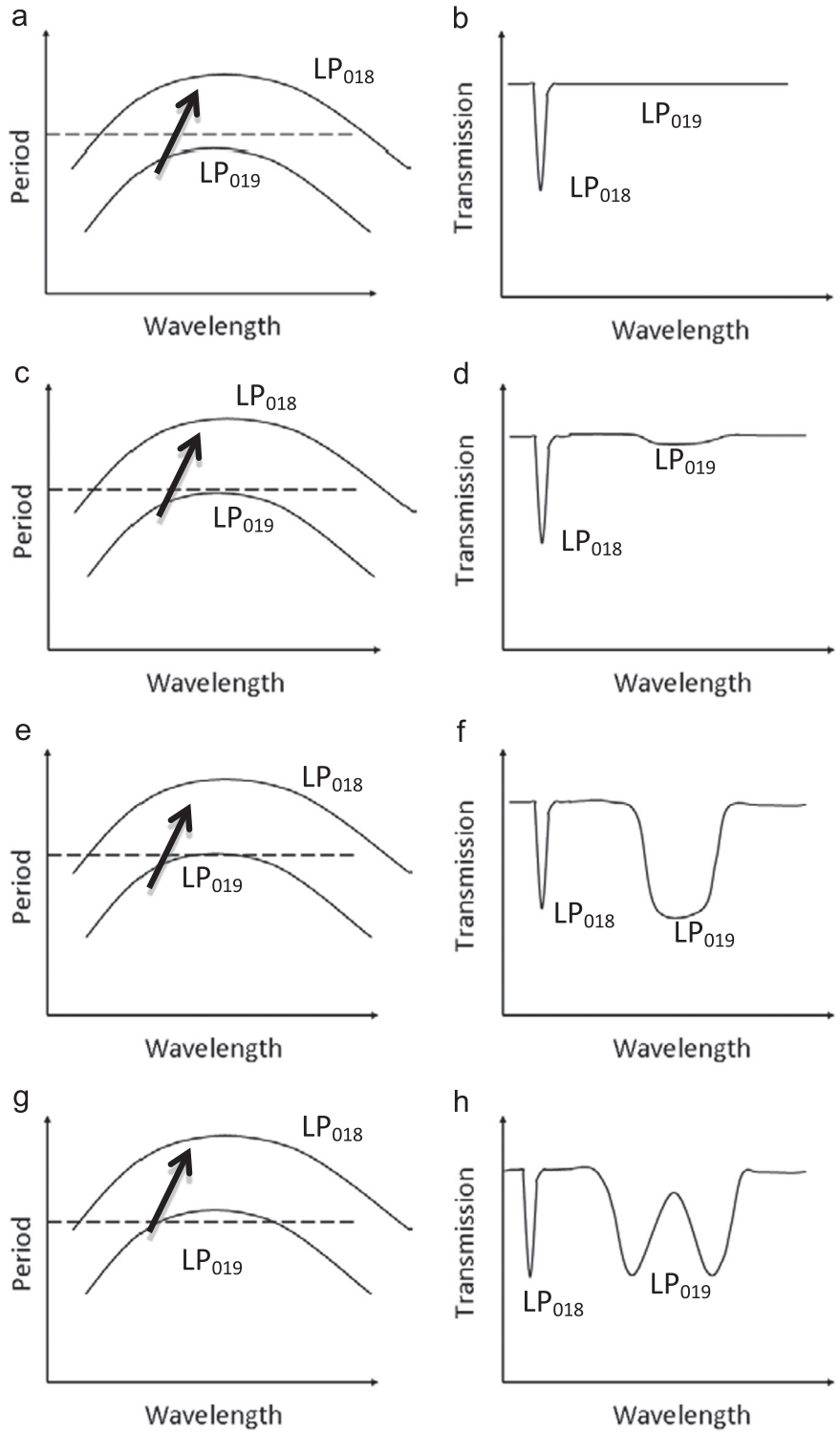

Fig. 2. Illustration of the properties of an LPG near the PMTP; arrow shows direction of the shift of the phase matching curve at the increase of the effective refractive index of the cladding mode caused by increasing optical thickness.

the core of the fibre, $n_{clad(i)}$ is the effective index of the LP_{0i} cladding mode and Λ is the period of the LPG. The phase matching condition described by Eq. (1) contains a turning point at which it has been shown (Cheung et al., 2008) that the sensitivity of the resonance band to perturbation of the surrounding environment is at its maximum.

For subsequent environmentally induced decreases in $(n_{core} - n_{clad(i)})$, the LPGs transmission spectrum is characterised by the formation of a broad resonance band that subsequently splits into two (Cheung et al., 2008). LPGs of appropriate period, coated with functional materials and operating at the PMTP, have been used to demonstrate sensors for chemical analytes in gaseous (Wang et al., 2013) or liquid media (Korposh et al., 2012a).

The PMTP phenomenon can be explained with reference to Fig. 2. In Fig. 2a, the grating period is such that phase matching to the 18th cladding mode (LP_{018}) is satisfied, but it is not possible to couple to the 19th cladding mode (LP_{019}), with a resulting LPG transmission spectrum of the form shown in Fig. 2b. Changes in

the optical thickness (product of the geometrical thickness and refractive index) of the coating cause an increase in the effective refractive index of the cladding modes. This causes the phase matching curves to change accordingly, "moving upwards" as illustrated in Fig. 2c, resulting in the development of a resonance band corresponding to coupling to the LP_{019} cladding mode, and a small blue-shift in the central wavelength of the LP_{018} resonance band. Further increases in the optical thickness of the coating result in conditions at which the coupling to the same cladding mode occurs at 2 different wavelengths leading to the further development of the LP_{019} resonance band, which subsequently splits into two bands, the so called dual resonance caused by the increase of the effective RI of the corresponding cladding mode.

2.2. LPG biosensor parameters

Typically, protein binding to the LPG surface follows the Langmuir isotherm theory that can be described by (Kinniburgh, 1986):

$$a = \frac{MkC}{1 + kC} \tag{2}$$

where a is the amount adsorbed, C is the solution concentration, M is the adsorption maximum and k is the equilibrium binding constant.

It can be assumed that the wavelength shift response of the biosensor is proportional to the adsorption (Chen et al., 2013) such that,

$$\Delta\lambda = \Delta\lambda_{max}\left(\frac{kC}{1 + kC}\right) \tag{3}$$

where $\Delta\lambda$ is the wavelength shift of the resonance band due to the refractive index change associated with the binding of the protein onto the self-assembled surface and $\Delta\lambda_{max}$ is the maximum wavelength shift due to complete formation of the protein layer.

In this work, the Langmuir isotherm is linearised using the *reciprocal* (*Langmuir*) in order to estimate the parameters k and $\Delta\lambda_{max}$ (Tellinghuisen, 2009; Maguis et al., 2008)

$$\frac{C}{\Delta\lambda} = \frac{1}{\Delta\lambda_{max}k} + \left(\frac{1}{\Delta\lambda_{max}}\right)C \tag{4}$$

The sensitivity (S) of the sensor for bio-molecule detection is given by (Barrios et al., 2008),

$$S = \frac{\Delta\lambda_{max}}{\sigma_{max}} \tag{5}$$

where σ_{max} is the surface density of the protein under detection (streptavidin) when all binding sites of the other immobilized molecule are occupied (biotin).

The theoretical detection limit of the sensor can also be estimated (Barrios et al., 2008)

$$D_{LS} = \frac{R}{S} \tag{6}$$

where R is the sensor resolution and S is the sensitivity (Eq. (5)).

3. Materials and methods

3.1. Material

Ethanol (99%), tetraethylorthosilicate (TEOS), Chloroauric acid ($HAuCl_4$), sodium borohydride ($NaBH_4$), potassium carbonate (K_2CO_3), Biotin (Molecular weight, ca. 244.31 g mol^{-1}) ((+)-Biotin N-hydroxysuccinimide ester), Streptavidin (M_w ca. 52.8 kDa) from Bacterium Streptomyces avidinii, were purchased from Sigma-Aldrich, UK. Ammonium hydroxide (NH_4OH 28%), Poly(allylamine hydrochloride) ($M_w \sim 58{,}000$, PAH) and 3-aminopropyltrimethoxysilane (APTES) were purchased from Sigma-Aldrich, UK. All reagents were of analytical grade and were used without further purification. Distilled water (with conductivity of 18.3 M cm) was obtained by reverse osmosis followed by ion exchange and filtration in a Millipore-Q (Millipore, Direct-QTM).

3.2. Synthesis of SiO_2:Au core/shell nanoparticles

SiO_2:Au core/shell NPs were made by first synthesising silica NPs using the Stober method (Stober et al., 1968) and then covalently attaching the Au NPs to the silica NPs surface to ensure stability. A solution of 7 mL of ethanol and 80 µl of TEOS was mixed with 3 mL of ammonium hydroxide for 15 min in a sonicator bath (to obtain ~300 nm diameter Si NPs). A solution of 22.5 mL of ethanol and 2 mL of TEOS was mixed with 3.5 mL of NH_4OH for 15 min in a sonicator bath (to obtain ~80 nm diameter Si NPs). The functionalisation of the silica NPs was carried out by adding 25 µl of 3-APTES to the reaction and leaving it to sonicate for an extra 15 min. The silica NPs were purified by centrifugation. The aqueous gold NPs (2–5 nm in diameter) solution was prepared using the methodology described by Bonnard et al. (1984). The solution of APTES-functionalised silica NPs was added dropwise to the solution of gold NPs in a volumetric ratio of 1:3 (SiO_2–NH_2:Au NPs) and stirred overnight (8 h) to provide stable covalent attachment of the Au NPs to the SiO_2 NPs.

3.3. LPG modification and characterisation

An LPG of length 40 mm and with a grating period of 110.7 µm was fabricated in boron–germanium co-doped optical fibre (Fibercore PS750, cut-off wavelength 670 nm) in a point-by-point fashion, side-illuminating the optical fibre by the output from a frequency-quadrupled Nd:YAG laser, operating at a wavelength of 266 nm. The transmission spectrum of the optical fibre was recorded by coupling the output from a tungsten-halogen lamp (Ocean Optics HL-2000) into the fibre and the transmitted light was analyzed using a fibre coupled CCD spectrometer (Ocean Optics HR4000). The grating period was selected such that the LPG operated at or near the PMTP, which, for coupling to a particular cladding mode (in this case LP_{019}), ensured optimised sensitivity (James and Tatam, 2006).

SiO_2:Au NPs were deposited onto the surface of the fibre using the LbL process and functionalised with biotin, as illustrated schematically in Fig. 3.

The surface of the section of the optical fibre containing the LPG was treated with a 1 wt% ethanolic KOH (ethanol/water=3:2, v/v) solution to terminate it with OH groups. The fibre was then immersed alternately into a 0.17 wt% solution containing a positively charged polymer, Poly(allylamine hydrochloride) PAH, and, after washing, into a 1 mg/mL solution containing the negatively charged SiO_2:Au NPs (80 or 300 nm in diameter), each for 15 min. This process was repeated until the required coating thickness was achieved, in this case after 3 deposition cycles. The coated fibre was then immersed in a 6.8 µM aqueous solution of biotin for 30 min to functionalise the SiO_2:Au NPs coating and to provide the sensor with its specificity to SV. The fibre was then rinsed in distilled water and dried by flushing with N_2 gas. The biotin remaining in the film was bound to the surface of each NP, which increased the surface area available for the binding of SV as compared to that available on a bare fibre. The presence of the functional chemical compounds coupled to the AuNPs increased the RI of the porous coating and resulted in a significant change in the LPG's transmission spectrum,

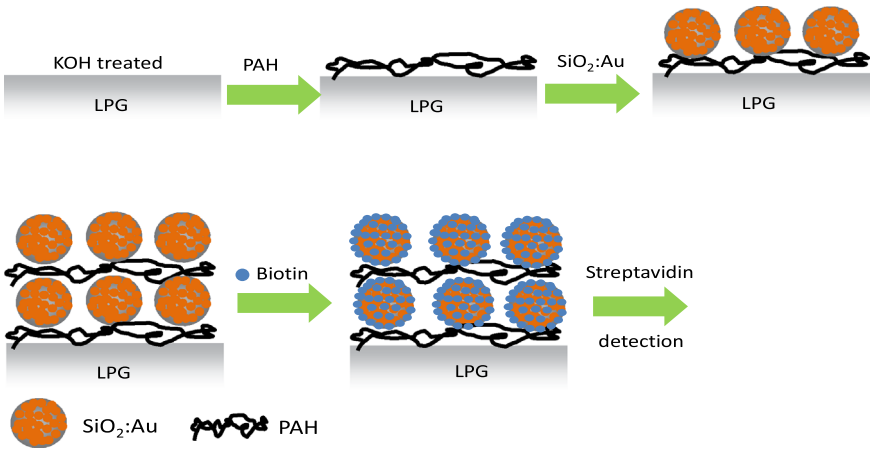

Fig. 3. Schematic illustration of the layer-by-layer deposition of a $(PAH/SiO_2:Au)_2$ film onto an optical fibre LPG.

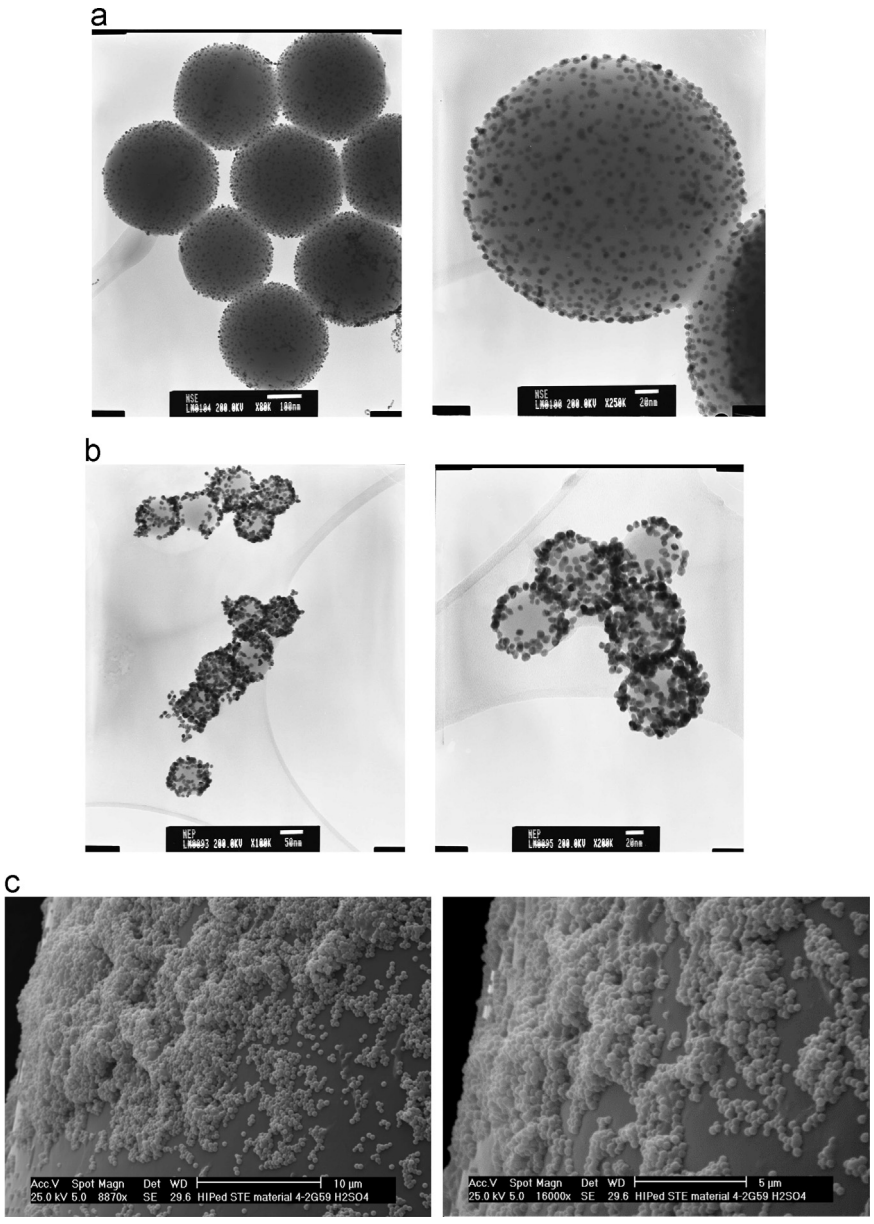

Fig. 4. TEM images of (a) 300 nm (scale bars: left hand, 100 nm and right hand, 20 nm) and (b) 80 nm (scale bars: left hand, 50 nm and right hand, 20 nm) SiO_2:Au NPs; and (c) SEM images of $(PAH/SiO_{2(300\ nm)}:Au)_3$ film deposited onto an optical fibre LPG (scale bars: left hand, 10 µm and right hand, 5 µm).

consistent with previous observations for increasing the optical thickness of coatings on LPGs.

3.4. Detection of streptavidin

For protein measurements, the $(PAH/SiO_2:Au)_3$-coated LPG was exposed to aqueous SV solutions of concentrations ranging from 19 nM to 2.7 μM. The sensor response was recorded at a frequency of 1 Hz. The transmission spectrum of the LPG was recorded in each analyte solution and also after washing and drying the LPG sensor. To avoid the effect of the bulk RI of the solution, the data were recorded in air after SV exposure and drying the LPG sensor. All experiments were conducted at 23 °C and 50% of relative humidity (RH). To study the effect of the Au on sensor performance, an LPG sensor modified with SiO_2 NPs, rather than with SiO_2 Au NPs, was also exposed to SV of different concentrations. SiO_2 NPs of different diameters were used to find the optimal conditions for sensor development. The sensitivity of the LPG sensor depends on the film thickness (Korposh et al., 2011) and porosity of the sensitive element. Two different diameters of SiO_2 NPs were chosen such that both parameters (porosity and film thickness) can be controlled simply by the choice of the appropriate SiO_2 NPs diameters.

3.5. TEM and SEM measurements

The SiO_2:Au NPs were imaged using a JOEL 2000 FX (200kv) (TEM). The morphology of the PAH/SiO_2:Au films were studied using a Philips XL 30 (SEM). The films deposited onto the optical fibre were coated with a thin (5 nm) platinum film using a Quorum Technologies SC 7640 Auto/Manual Sputter Coater to allow electrical discharge of the sample surface during the interaction with the electron beam.

4. Results and discussion

4.1. LPG modification

Fig. 4a and b shows TEM images that demonstrate successful modification of the SiO_2 NPs of 300 and 80 nm diameter respectively with the Au NPs. The Au NPs provide the surface for the deposition of biotin that produces a change in the RI upon future immobilisation of SV molecules. Fig. 4c shows the SEM image of the LPG optical fibre with the $(PAH/SiO_{2(300\ nm)}:Au)_3$ film successfully assembled onto the fibre. Complete surface coverage was not achieved most likely owing to the presence of NH_2 functional groups on the SiO_2 NPs that promoted some repulsive charge effects with the PAH and an incomplete aggregation reaction between the polyelectrolyte and the fibre surface. As will be shown later, this surface coverage was sufficient to conduct measurements of the binding between biotin and streptavidin.

Fig. 5a–c shows the transmission spectra of the LPG measured in water and air after the deposition of the $(PAH/SiO_{2(300\ nm)}:Au\ NPs)_3$ film and after the binding of biotin, respectively. Similar to

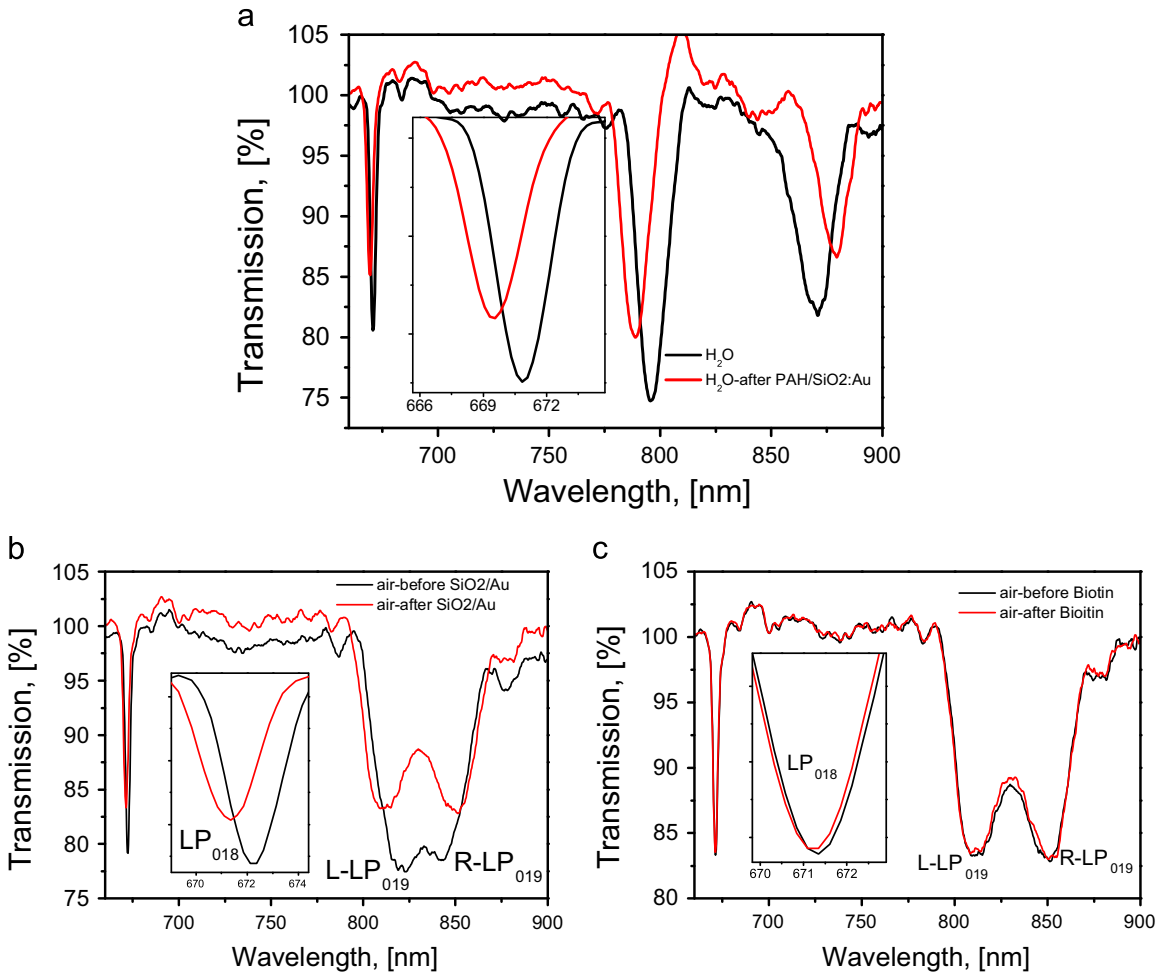

Fig. 5. (a) The transmission spectrum of an LPG of period 110.7 μm, measured with the LPG in water and (b) in air: black line, before and red line, after $(PAH/SiO_{2(300\ nm)}:Au)_3$ film deposition; and (c) transmission spectrum of the LPG coated the $(PAH/SiO_{2(300\ nm)}:Au)_3$ film, measured with the LPG in air: black line before and red line, after biotin deposition. (For interpretation of the references to colour in this figure legend, the reader is referred to the web version of this article.)

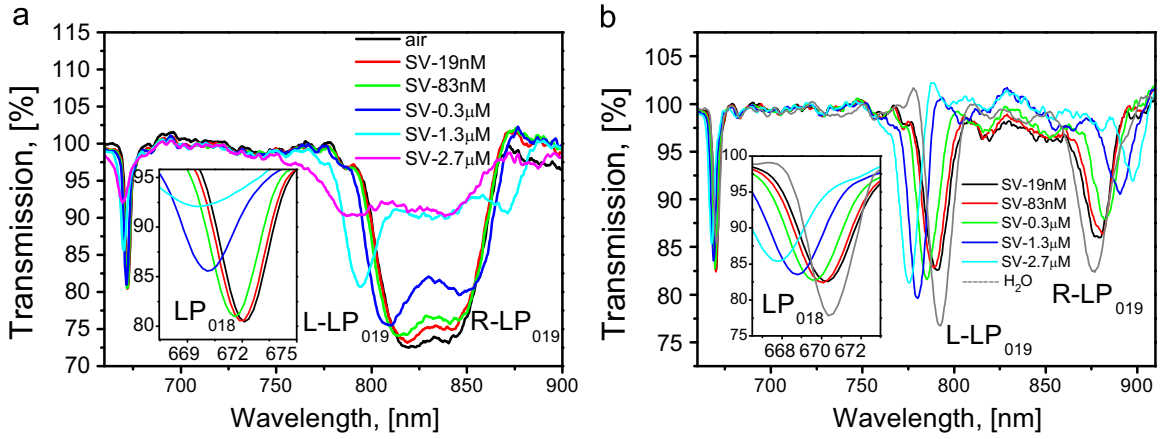

Fig. 6. Transmission spectrum of the $(PAH/SiO_{2(300\ nm)}:Au)_3$ coated LPG modified on exposure to SV of different concentrations in: (a) air and (b) aqueous solution.

observation of other LPG based chemical sensors (DeLisa et al., 2000), the first resonance band (@ ca. $\lambda = 670$ nm), corresponding to coupling to the LP_{018} cladding mode, exhibited blue wavelength shifts of ca. 1 nm and ca. 0.11 nm for $(PAH/SiO_2:Au\ NPs)_3$ film and biotin deposition, respectively. The second resonance band (@ ca. $\lambda = 830$ nm), corresponding to coupling to the LP_{019} cladding mode at the PMTP, exhibited wavelength shifts of 14 nm and 10 nm for $L\text{-}LP_{019}$ and $R\text{-}LP_{019}$, after PAH/SiO_2:Au NPs film deposition as shown in Fig. 5b. These results indicate successful deposition of the PAH/SiO_2:Au NPs film onto the LPG, confirming the SEM results (Fig. 4c).

The small wavelength shift observed after biotin adsorption, visible in Fig. 5c, most likely relates to the small RI change induced by the biotin molecule. After deposition of the $(PAH/SiO_2:Au\ NPs)_3$ film and functionalisation with biotin, the LPG sensor was exposed to SV solutions of different concentrations.

4.2. StreptavIDIn detection

Fig. 6a and b shows the changes in the transmission spectrum of the LPG sensor modified with the $(PAH/SiO_{2(300\ nm)}:Au)_3$ film upon exposure to aqueous solutions of SV of different concentrations,

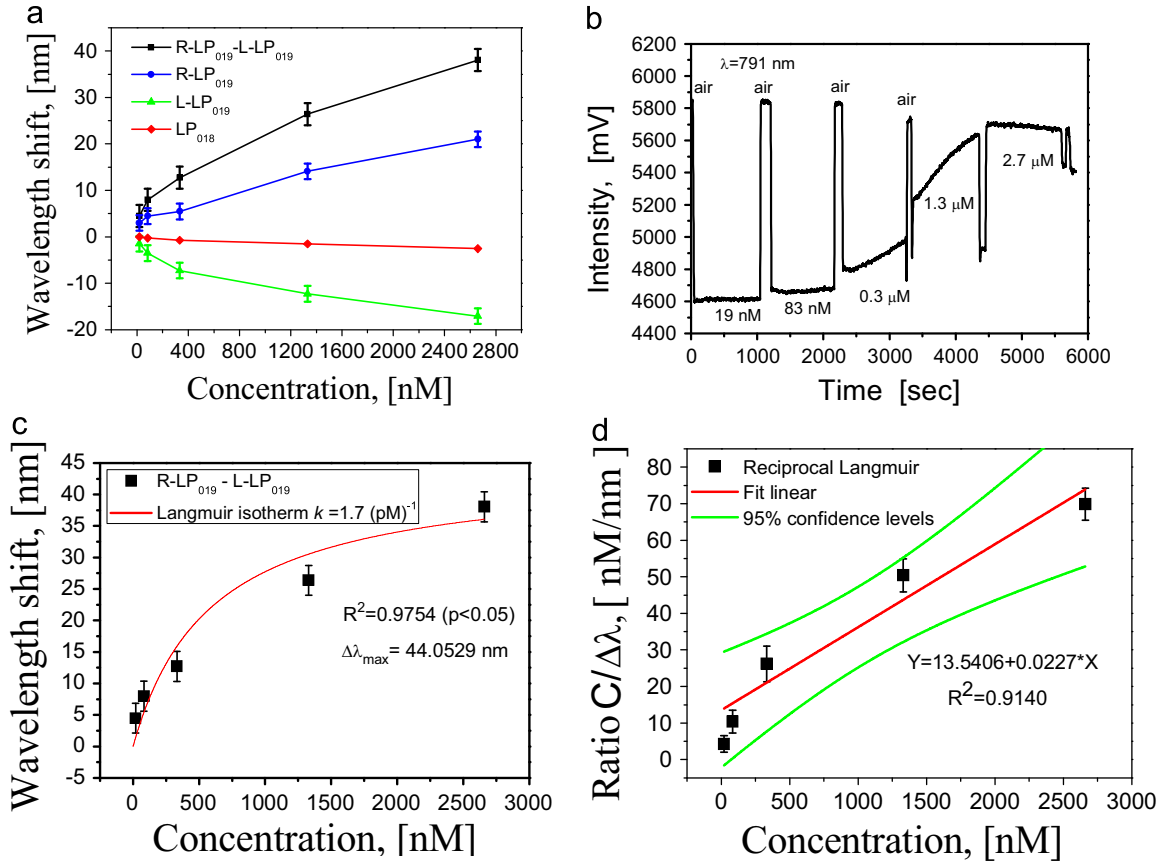

Fig. 7. (a) Concentration dependence of the wavelength shift derived from the data shown in Fig. 6a; squares, wavelength differences between $R\text{-}LP_{019}$ and $L\text{-}LP_{019}$ resonance bands; circles, $R\text{-}LP_{019}$ band; triangles, $L\text{-}LP_{019}$ resonance band; and diamonds, LP_{018} resonance band. (b) The change in transmission of the device measured at a wavelength of 791 nm on immersion into solutions of different SV concentration. (c) Langmuir isotherm fit of data from Fig. 7a and (d) linearization of Langmuir isotherm (Fig. 7c) using Eq. (4). The error bars represent the standard deviation of 5 blank measurements and the green lines provide the confidence level (Belter et al., 2014; Loock and Wentzell, 2012). (For interpretation of the references to colour in this figure legend, the reader is referred to the web version of this article.)

obtained by removing, washing and drying the LPG after each exposure, measured in air and in solution, respectively. Similar to the binding of the SiO_2 NPs and biotin (Fig. 5), the adsorption of the SV leads to a blue wavelength shift of the first resonance band LP_{018} (@ ca. λ=670 nm) and wavelength shifts for L-LP_{019} and R-LP_{019}. However, the magnitude of the change at the adsorption of the SV was significantly different. In particular, the LP_{018} band shifted by ca. 3 nm for measurements both in air and in solution, while much greater changes of ca. 17 and 31 nm for L-LP_{019} and 21 and 32 for R-LP_{019} when measured in solution and in air, respectively. The wavelength shift at the SV binding is 30 times greater as compared to the change caused by the biotin adsorption. This most plausibly is owing to the RI difference between two compounds; the SV is much larger (52.8 kDa) as compared to the biotin (244.31 g mol^{-1}) and hence causes the higher RI change when adsorbed onto the surface of the LPG sensor. It should be noted that the difference between values obtained when measured in the solution and in the air is related to the bulk RI values 1.33 and 1.00, respectively; the LPG with the current grating period operates closer to the PMTP at the bulk RI=1 and hence has higher sensitivity in air than in solution.

Fig. 7 shows the effect of SV configuration on different parameters. Fig. 7a shows the wavelength shift of different peaks for both absolute and relative positions with the difference between the centre wavelengths of the R-LP_{019} and L-LP_{019} resonance bands showing the highest sensitivity. Fig. 7b shows intensity against time as the sensor is inserted into different SV concentrations, with discontinuities observed when the sensor is removed from SV due to the bulk RI change between air (n=1) and water (n=1.33) and is not related to the protein binding. Fig. 7(c) shows a fit of the Langmuir isotherm (Eq. (3)) to the adsorption of SV to the biotin (Kinniburgh, 1986; Maguis et al., 2008; Chen et al., 2013). Fig. 7(d) shows the linearised form of the fit (Eq. (4)). The maximum wavelength shift and binding constant were 44.05 nm and 1.7 $(pM)^{-1}$ (Fig. 7c), respectively, when the difference between the centre wavelengths of the R-LP_{019} and L-LP_{019} resonance bands (Fig. 6a and b) was considered. The response time for lower SV concentrations (up to 83 nM) was of the order of several seconds, suggesting the completion of SV binding to the biotin (Fig. 7b). For higher concentrations, however, the response time was much slower and was not complete within 15 min for SV concentration ranging from 0.3 to 2.7 μM possibly owing to the physical adsorption of the SV to SiO_2 NPs. This phenomenon needs further experimental investigation and will be explored in future work.

The theoretical surface density of streptavidin monolayer is 6. 4 $^{ng}/_{mm^2}$ as calculated from the average length of a streptavidin molecule (P_{SV}) (Li et al., 2004; Barrios et al., 2008; Maguis et al., 2008; Chen et al., 2013).

Therefore, the sensitivity of the proposed sensor LPG coated with $(PAH/SiO_{2(300\ nm)}:Au)_3$ is 6.9 nm/(ng/mm^2), where the maximum wavelength shift was determined by the reciprocal Langmuir transformation of the Langmuir isotherm, Fig. 7d.

The theoretical detection limit of the proposed sensor was 19 pg/mm^2 estimated using Eq. (6) using the following parameters: S = 6.9 nm/(ng/mm^2) and R = 0.13 nm is the spectrometer resolution if the environmental noise and the inherent thermal noise of the

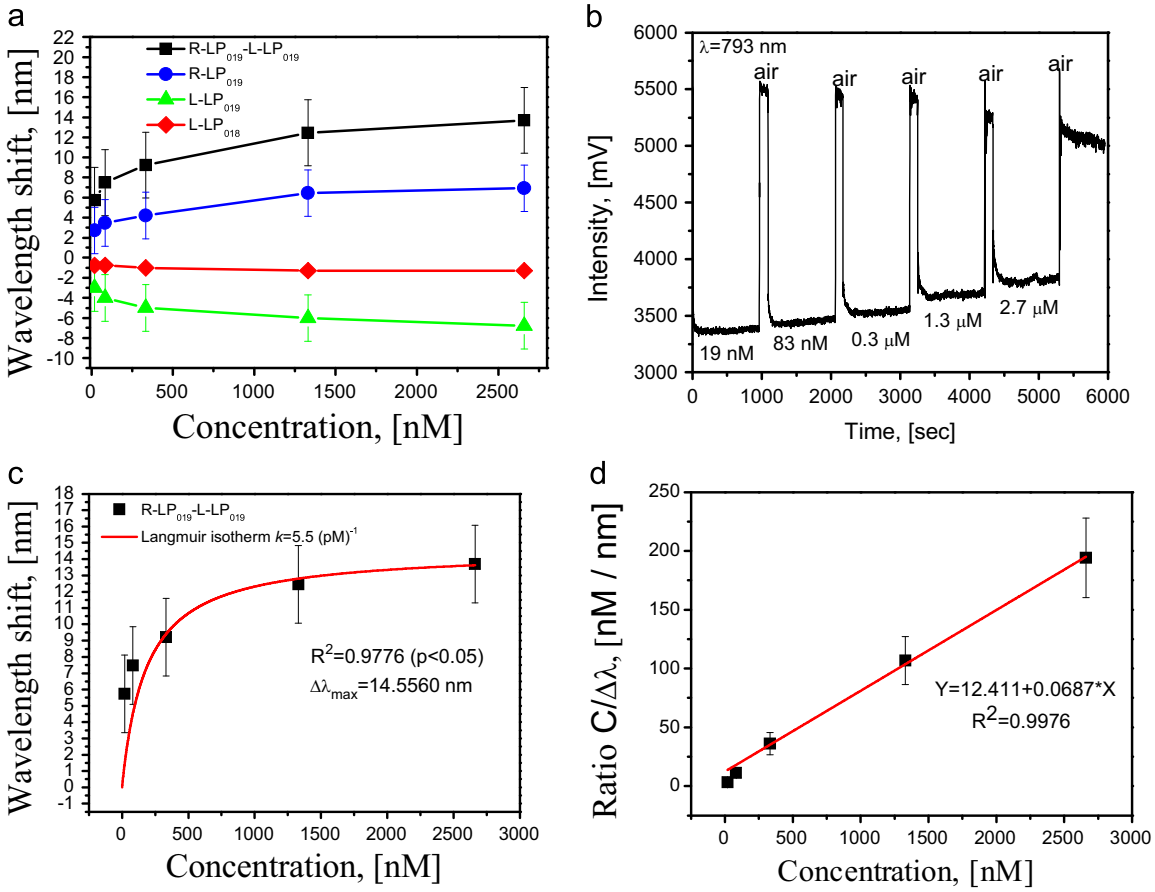

Fig. 8. (a) Concentration dependence of the wavelength shift derived; squares, wavelength differences between R-LP_{019} and L-LP_{019} resonance bands; circles, R-LP_{019} band; triangles, L-LP_{019} resonance band; and diamonds, LP_{018} resonance band. (b) The change in transmission of the device measured at a wavelength of 793 nm on immersion into solutions of different SV concentration and using SiO_2 NPs of diameter 80 nm. (c) Langmuir isotherm fit of data (d) linearization of Langmuir isotherm using Eq. (4).

spectrometer are neglected (Chen et al., 2013; Barrios et al., 2008).

4.3. Effect of SiO_2 NP diameter

Fig. 8 shows the same format of results as Fig. 7 but for a film comprised of 80 nm diameter SiO_2 NPs. Similar spectral changes to those observed with the $(PAH/SiO_{2(300\ nm)}:Au\ NPs)_3$ film (Fig. 5) were observed on the deposition of $(PAH/SiO_{2(80\ nm)}:Au\ NPs)_3$ mesoporous thin film and biotin (Fig. S1). The amplitude of the change, however, was considerably smaller when 80 nm diameter SiO_2 NPs were used (Figs. 7a, 8a and S2) demonstrating that the sensor with larger SiO_2 NPs has higher sensitivity. This can be attributed to the thinner film (total thickness of ca. 240 nm) deposited onto the LPG when 80 nm diameter SiO_2 NPs were used as compared to 300 nm diameter SiO_2 NPs (total thickness of ca. 900 nm) which resulted in reduced efficiency of the evanescent wave interaction with the $(PAH/SiO_{2(80\ nm)}:Au\ NPs)_3$ film. It was previously demonstrated that LPG sensor performance strongly depends on film thickness (Korposh et al., 2011). In addition, the 300 nm diameter SiO_2 NPs, enhance the adsorption of more protein since they have higher gold content and at this layer thickness greater diffusion between the interspace of the NP assembly complex is enabled.

In addition, the completion of SV binding to biotin is faster when the SiO_2 NPs are smaller (Figs. 7b and 8b). Nonetheless, the slowest response time of ca. 10 min for concentrations ranging from 0.3 to 2.7 μM occurred when the SiO_2 NPs of 300 nm were used. This aspect requires further experiments in order to investigate whether there is direct and stronger physical adsorption of the SV to the SiO_2 NPs when the NPs are larger.

Using the data in Fig. 8c and d, the binding constant and maximum wavelength shift for the LPG fibre coated with $(PAH/SiO_{2(80/\ nm)}:Au)_3$ thin film was 5.5 $(pM)^{-1}$ and 14.56 nm, respectively. The sensitivity and limit of detection were 2.27 $nm/\left(ng/mm^2\right)$ and 57 pg/mm^2 (neglecting experimental noise). These parameters indicate that the sensitivity of the sensor modified with the $(PAH/SiO_{2(80\ nm)}:Au)_3$ thin film is ca 3 times lower than the sensitivity of the sensor with $(PAH/SiO_{2(300\ nm)}:Au)_3$ thin film.

The sensitivity of the LPG modified with the $(PAH/SiO_2:Au\ NPs_{300})_3$ thin film is at least two orders of magnitude greater than previously reported optical fibre streptavidin bio-sensors, Table 1 (DeLisa et al., 2000; Pilla et al., 2012; Wang et al., 2009; Maguis et al., 2008).

This is due to both the high porosity of the sensitive layer and the enhanced RI sensitivity due to the use of Au NP coated SiO_2 NPs.

The LoD of the proposed sensor will dictate the range of applications. For instance, detection of the drugs (vancomycin) in blood requires a detection level of mM (Korposh et al., 2014). Some proteins such as serum albumin and interleukin 6 in blood require a dynamic range of concentration ranging from tens of mg/mL to pg/mL, respectively (Anderson and Anderson, 2002).

The streptavidin–biotin interaction was used as a model system to characterise influence of the novel coating structure on the LPG sensor performance, since the properties of the biotin–streptavidin interaction are well known. Experiments with the clinically relevant proteins and real samples are underway and will use the characterisation information provided from the streptavidin experiments.

To extend the range of applications, the performance of the proposed biosensor will need to be further enhanced by addressing the following:

(1) Enhance the LPG surface coverage: as can be seen from SEM images (Fig. 4b) the coverage of the $(PAH/SiO_2:Au\ NPs_{300})_3$ thin film of the LPG surface is not uniform. This can be improved by modifying the deposition procedure of the SiO_2 NPs by increasing the efficiency of the SiO_2 adsorption via SiO_2 NPs surface modification. Studies are currently ongoing to modify the SiO_2 NPs surface with a higher number of ligands that will intensify the negative charge of the NPs before assembly over the fibre coated with PAH.
(2) Enhance the coverage of the SiO_2 with Au NPs. A higher rate of Au NPs can be assembled over the SiO_2 surface. This can be improved by modifying the initial procedure used to synthesise the SiO_2:Au NPs.
(3) Optimising grating period such that sensor operates closer to the PMTP, which is known to give higher sensitivity to the analyte (Cheung et al., 2008); and optimising film thickness by studying the effect of the number of layer for smaller SiO_2 NPs diameter that might increase the specific surface area hence enhance the efficiency of light interaction with analyte. The latter however depends also on the SiO_2 NPs surface coverage by the Au NPs. Preliminary results obtained by optimising the grating period (Fig. S3) demonstrated that SV with concentration of 2.5 nM can be detected using the LPG sensor modified with the $(PAH/SiO_{2(80\ nm)}:Au)_3$ thin film.
(4) Test protein solutions comprised not only of SV molecules, but also other interfering molecules. The study presented here showed the selectivity and performance for SV detection but a more challenging matrix of analytes is required to further establish the selectivity to its bio-targets. Initial studies will be carried out with SV mixed with different proteins before selecting a relevant clinical biomarker to immobilise over the SiO_2:Au NPs sensors to enable the analysis to be moved to physiological conditions.

5. Conclusion

An LPG coated with a $(PAH/SiO_2:Au\ NPs)_3$ film and functionalised with biotin was used as a sensor for the detection of

Table 1
Grating based optical fibre bio-sensors and their limit of detection.

References	Type of film	Sensitivity/type of protein	Limit of detection
DeLisa et al. (2000)	Antibody	Anti-IgG	0.7 (μg/mL)
Maguis et al. (2008)	Poly-ethylene-imine (PEI)/dextran sulphate sodium (DSS)	Extravidin(Anti-BSA) 0.788–0.835×10^{-6} r.i.u. mm^2/pg	12–13 pg/mm^2
Pilla et al. (2012)	Atactic polystyrene (PS)	Anti-IgG	~5 pg/mm^2
Wang et al. (2009)	Poly(allylamine hydrochloride) (PAH)/poly{1-[4-(3-carboxy-4-hydroxyphenylazo)-benzensulfonamido]-1,2-ethanediyl, sodium salt} (PCBS)	Biotin–streptavidin	<0.0125 mg/mL
Carrasquilla et al. (2011)	Sol–gel-AuNPs with biotin streptavidin	Adenosine triphosphate	400 μM
Huang et al. 2013	Nano iron and silica particles	pH	0.66 nm/pH
Developed sensor	Silica core gold shell (SiO_2:Au) NPs	Biotin–streptavidin	0.000195 mg/mL 19 pg/mm^2

streptavidin protein. A curve fit of the response of the proposed sensor LPG coated with $(PAH/SiO_{2(300\ nm)}:Au)_3$ to SV concentration (Fig. 7a) using Langmuir isotherm theory demonstrated a maximum wavelength shift and binding constant of 44.05 nm and 1.7 $(pM)^{-1}$ with a sensitivity of 6. 88 $nm/\left(ng/mm^2\right)$ and theoretical limit of detection of 19 pg/mm^2 (neglecting experimental noise). The sensitivity of the LPG modified with the $(PAH/SiO_{2(80\ nm)}:Au)_3$ thin film is ca 3 times lower than sensitivity of the sensor with $(PAH/SiO_{2(300\ nm)}:Au)_3$ thin film. The properties of the proposed sensor can be tailored simply by changing the ligand, which allows the targeting of clinically relevant protein compounds.

Acknowledgements

We would like to thank the Engineering and Physical Sciences Research Council (EPSRC), UK, for supporting this work via Grants EP/H02252X and EP/L010437. For enquiries relating to access to the research data or other materials referred to in this article, please contact Cranfield University Library and Information Services – library@cranfield.ac.uk. The authors would like also to acknowledge the support of the EPSRC EP/G061661/1 Advanced Ultrasonics Platform grant, the University of Nottingham, Dean of Engineering Faculty Award (ENG763) and National Council of Science and Technology of Mexico (CONACyT) and the Ministry of Public Education in Mexico (DGRI-SEP).

Appendix A. Supplementary material

Supplementary data associated with this article can be found in the online version at http://dx.doi.org/10.1016/j.bios.2015.08.046.

References

Anderson, N.L., Anderson, N.G., 2002. Mol. Cell. Proteom. 1 (11), 845–867.
Bandara, A.B., Zuo, Z., Ramachandran, S., Ritter, A., Heflin, J.R., Inzana, T.J., 2015. Biosens. Bioelectron. 70, 433–440.
Barrios, C.A., Banuls, M.J., González-Pedro, V., Gylfason, K.B., Sánchez, B., Griol, A., Maquieira, A., Sohlstrom, H., Holgado, M., Casquel, R., 2008. Opt. Lett. 33, 708–710.
Belter, M., Sajnóg, A., Baralkiewicz, D., 2014. Talanta 129, 606–616.
Bonnard, C., Papermaster, D.S., Kraehenbuhl, J.-P., 1984. The streptavidin-biotin bridge technique: application in light and electron microscope immunocytochemistry. In: Polak, J.M., Varndell, I.M. (Eds.), Immunolabelling for Electron Microscopy. Elsevier, New York, pp. 95–111.
Carrasquilla, C., Xiao, Y., Xu, C.Q., Li, Y., Brennan, J.D., 2011. Anal. Chem. 83, 7984–7989.
Chen, L.H., Chan, C.C., Ni, K., Hu, P.B., Li, T., Wong, W.C., Balamurali, P., Menon, R., Shaillender, M., Neu, B., Poh, C.L., Dong, X.Y., Ang, X.M., Zu, P., Tou, Z.Q., Leong, K.C., 2013. Sens. Actuators B: Chem. 178, 176–184.
Cheung, S.C., Topliss, S.M., James, S.W., Tatam, R.P., 2008. J. Opt. Soc. Am. B. 25, 897–902.
DeLisa, M.P., Zhang, Z., Shiloach, M., Pilevar, S., Davis, C.C., Sirkis, J.S., Bentley, W.E., 2000. Anal. Chem. 72, 2895–2900.
Grattan, K., Meggitt, B., 1999. Chemical and Environmental Sensing. Kluwer Acad. Publisher, Boston.
Homola, J., 2008. Chem. Rev. 108, 462–493.
Huang, Y., Gao, Z., Chen, G., Xiao, H., 2013. Smart Mater. Struct. 22, 075018 8 p.
James, S., Tatam, R., 2006. J. Opt. A: Pure Appl. Opt. 8, S430.
James, S.W., Tatam, R.P., 2003. Meas. Sci. Technol. 14, R49.
Kinniburgh, D.G., 1986. Environ. Sci. Technol. 20, 895–904.
Kodaira, S., Korposh, S., Lee, S.-W., Batty, W. J., James, S. W., Tatam, R. P., 2008. In: Proceedings of the 3rd International Conference on Sensing Technology, ICST 2008, pp. 481–485.
Korposh, S., Lee, S.-W., James, S.W., Tatam, R.P., 2011. Meas. Sci. Technol. 22 (075208) 10 p.
Korposh, S., Selyanchyn, R., Yasukochi, W., Lee, S.-W., James, S., Tatam, R., 2012a. Mater. Chem. Phys. 133, 785–792.
Korposh, S., James, S., Tatam, R., Lee, S.-W., 2012. Optical fibre long-period gratings functionalised with nano-assembled thin films: approaches to chemical sensing. In: Cuadrado-Laborde (Ed.), Current Trends in Short-and Long-Period Gratings. InTech, Croatia, pp. 237–2264.
Korposh, S., Chianella, I., Guerreiro, A., Caygill, S., Piletsky, S.A., James, S.W., Tatam, R.P., 2014. Analyst. 139, 2229–2236.
Li, H., Ha Park, S., Reif, J.H., LaBean, T.H., Yan, H., 2004. J. Am. Chem. Soc. 126, 418–419.
Loock, H.P., Wentzell, P.D., 2012. Sens. Actuators B: Chem. 173, 157–163.
Maguis, S., Laffont, G., Ferdinand, P., Carbonnier, B., Kham, K., Mekhalif, T., Millot, M. C., 2008. Opt. Express 16, 19049–19062.
Marques, L., Hernandez, F.U., Korposh, S., Clark, M., Morgan, S., James, S.W., Tatam, R.P., 2014. Proc. SPIE 9157, 91574S.
Mishra, V., Singh, N., Tiwari, U., Kapur, P., 2011. Sens. Actuators A 167, 279–290.
Orgovan, N., Peter, B., Bosze, S., Ramsden, J.J., Szabo, B., Horvath, R., 2014. Sci. Rep. 4 (4034) 8 p.
Patko, D., Cottier, K., Hamori, A., Horvath, R., 2012. Opt. Express, 20 (21), pp. 23162–23173. Physics, 133, 784–782.
Pilla, P., Sandomenico, A., Malachovská, V., Borriello, A., Giordano, M., Cutolo, A., Ruvo, M., Cusano, A., 2012. Biosens. Bioelectron. 31 (1), 486–491.
Stober, W., Fink, A., Bohn, E., 1968. J. Colloid Interface Sci. 26, 62–69.
Tellinghuisen, J., 2009. Methods Enzymol. 467, 499–529.
Wang, T., Korposh, S., James, S., Tatam, R., Lee, S.-W., 2013. Sens. Actuators B: Chem. 185, 117–124.
Wang, Z., Heflin, J.R., Van Cott, K., Stolen, R.H., Ramachandran, S., Ghalmi, S., 2009. Sens. Actuators B 139, 618–623.
Wulfkuhle, J.D., Liotta, L.A., Petricoin, E.F., 2003. Nat. Rev. Cancer. 3, 267–275.